COBEM 2023 27TH INTERNATIONAL CONGRESS OF MECHANICAL ENGENEERING

ABCM Brazilian Society of Mechanical Sciences and Engineering
27th ABCM International Congress of Mechanical Engineering
December 04-08, 2023, Florianópolis-SC, Brazil

COB-2023-1061
A COMPARISON BETWEEN POROUS AND FREE-FLOW MEDIA USING THE FINITE ELEMENT METHOD TO SOLVE THE GENERALIZED DARCY/FORCHHEIMER EQUATION

João P. I. Souza
Gustavo R. Anjos
Universidade Federal do Rio de Janeiro
jpisouza@mecanica.coppe.ufrj.br
gustavo.rabello@coppe.ufrj.br

Abstract. *The current study aims at simulating flows in both free-flow and porous regions. The discretization of mass and momentum equations, using the Finite Element Method (FEM), are presented. Also, the semi-lagrangian technique, where unconditional stability is successfully achieved for the numerical solution in different geometries, is developed. For porous and conjugated flows, the Darcy-Forchheimer term is included in the classical Navier-Stokes equation, so that the resistance imposed by the porous medium is considered in the pressure gradient. A second-order spatial convergence is assured for velocity and temperature fields, since a quadratic + linear pair of triangle mesh elements is used, fulfilling the well-known LBB condition. The MINI element is used to verify the results with the literature as well. Energy balance is also made in this work, so that the temperature field can be determined along the domain, evidentiating the differences between free-flow and porous domains with respect to not only pressure and velocity field distribution but also how the medium interferes with heat transfer phenomena. A benchmark validation for the finite element method applied to fluid mechanics is provided and the well-known case of Poiseuille flow is simulated using both media in order to compare the pressure along the channel for the two cases. As expected, a porous medium imposes a higher pressure gradient on the flow, but with lower values for the velocity field. The mass flow for both cases is the same, but a flatter curve is observed in the porous domain due to the effects imposed by the resistance of the medium. Graphical results are shown to illustrate and compare all the cases simulated in this work.*

Keywords: *FEA, CFD, porous medium, semi-Lagrangian, unstructured mesh, Python*

1 INTRODUCTION

The present work is intended to numerically analyze conjugated flows and compare them with free-flow systems. For numerical simulation, the Navier-Stokes, coupled with the Darcy-Forchheimer equation for porous media, provides good results for conjugated fluid flows, as seen in Souza and Anjos (2023). The formulation will be treated through the Euler approach and its governing equations for mass and momentum conservation will be discretized to simulate the complete phenomenon. The Finite Element Analysis (FEA) is then applied to the governing equation so that a computational solution can be obtained. The implementation is then made through *Python*'s scientific language and the open source software *Gmsh* was used for mesh generation.

It is important to discuss a few of the methods used to solve systems of partial differential equations. Bessaih *et al.* (2018) proposed a technique for the three-dimensional Navier-Stokes system of equations, which must be solved for some detailed cases, where the two-dimensional approach will not satisfy all the requisites. This technique consists of introducing a delay in the non-linear term (responsible for the advective phenomenon), which, according to Bessaih *et al.* (2018), "introduces a regularizing effect in the equations and allows to prove the uniqueness of weak solutions". Abdelwahed *et al.* (2011) analyze the two-dimensional form of the Navier-Stokes equations and proposes the use of the finite element method to find a solution for them. For that, Abdelwahed *et al.* (2011) use the stream function (ψ) and vorticity (ω) in the z direction formulation, modifying the set of equations to the vorticity form. Toro *et al.* (2018) also make use of the finite element technique, providing examples of both flow and heat transfer phenomena. In this case, instead of using stream function vorticity, the authors simulate a potential flow, therefore an ideal fluid, around a cylinder.

For porous region analysis, the reference used is the work developed by Cimolin and Discacciati (2013), where the Darcy/Forchheimer formulation is presented. The models described by the authors are the Navier-Stokes/Darcy (NSD) model, the Navier–Stokes/Forchheimer (NSF) model and the Penalization (PE) model. As for the PE model, which is the method used here to describe conjugated regions, the whole domain is described with a single equation of momentum conservation, which simplifies the solver. The PE method is a good approximation of the physical problem discussed here since the interface is of low interest for the purpose of this work. A similar approach is also used by Mesquida (2019), who makes use of CFD software to simulate a gasoline particle filter, using the Reynolds Average Numerical solution,

also referred to as RANS, approach for turbulent regimes.

2 GOVERNING EQUATIONS

The partial differential equation for the linear momentum balance, including the constitutive equation for Newtonian incompressible fluids, is given by Eq. (1), known as the Navier-Stokes equation, as presented by Batchelor (2000).

$$\frac{\partial \mathbf{u}_D}{\partial t_D} + \mathbf{u}_D \cdot \nabla \mathbf{u}_D = -\frac{1}{\rho}\nabla p_D + \nu \nabla^2 \mathbf{u}_D + \mathbf{g}_D, \tag{1}$$

where $\mathbf{u}$ is the velocity vector field, p the pressure field, ν the kinematic viscosity and $\mathbf{g}$ the gravitational field. The non-dimensional variables are defined as follows, where the subscript D indicates the dimensional variable and L and U are the characteristic length and velocity, respectively:

$$\mathbf{x} = \frac{\mathbf{x}_D}{L}, \quad \mathbf{u} = \frac{\mathbf{u}_D}{U}, \quad t = \frac{t_D U}{L}, \quad \mathbf{g} = \frac{\mathbf{g}_D}{|\mathbf{g}_{ref}|}, \quad p = \frac{p_D}{\rho U^2}. \tag{2}$$

The continuity equation (Eq. (3)) and the momentum equation for porous media (Eq. (4)), known as Darcy/Forchheimer equation, in their non-dimensional form, can be found by replacing the correlations above in the original dimensional equations:

$$\nabla \cdot \mathbf{u} = 0, \tag{3}$$

$$\frac{D\mathbf{u}}{Dt} + \frac{\varphi}{ReDa}\left(\mathbf{u} + Fo\varphi|\mathbf{u}|\mathbf{u}\right)\varepsilon = -\nabla p + \frac{1}{Re}\nabla^2 \mathbf{u} + \frac{1}{Fr^2}\mathbf{g}, \tag{4}$$

where φ is the porosity of the medium and ε defines if the region is either porous, assuming the value of 1, or not, with a null value. $Re = UL/\nu$ is known as the Reynolds number, $Da = K/L^2$ is the Darcy number, $Fo = \rho C_F \sqrt{K} U/\mu$ the Forchheimer number and $Fr = U/\sqrt{gL}$ the Froude number. K is the permeability coefficient, C_F is the inertial resistance, μ the dynamic viscosity and g the absolute value of the gravitational field.

Equation (5) is obtained through energy balance and can be solved to find the temperature of a Newtonian incompressible fluid, applying Fourier's law for heat conduction, with the dimensionless temperature $T = (T_{in} - T_D)/(T_{in} - T_s)$.

$$\frac{\partial T}{\partial t} + \mathbf{u} \cdot \nabla T = \frac{1}{RePr}\left(\nabla^2 T\right). \tag{5}$$

Here $Pr = \nu/\alpha$ is the Prandtl number, where α is the thermal diffusivity.

3 THE FINITE ELEMENT METHOD

In this section, the variational and the discrete forms will be shown for the Navier-Stokes equation and, then, the Darcy/Forchheimer terms will be added to the final linear system of equations.

3.1 The Variational Form

According to Zienkiewicz and Taylor (2000), the weak form, also known as variational form, is obtained by multiplying each of the governing equations by the weight functions w, q and r, associated with velocity, pressure and temperature,

respectively. The Green theorem is applied to the second-order and pressure gradient terms. Since, in this work, all boundary conditions are either Dirichlet or null Neumann, the boundary integral resulted from such theorem is null and the final variational form is given by:

$$\int_\Omega \frac{D\mathbf{u}}{Dt} \cdot \mathbf{w} d\Omega + \int_\Omega \frac{\varphi\varepsilon}{ReDa} (\mathbf{u} + Fo\varphi|\mathbf{u}|\mathbf{u}) \cdot \mathbf{w} d\Omega = \int_\Omega p\nabla \cdot \mathbf{w} d\Omega - \frac{1}{Re} \int_\Omega (\nabla \mathbf{u} : \nabla \mathbf{w}) \, d\Omega + \int_\Omega \frac{1}{Fr^2} \mathbf{g} \cdot \mathbf{w} d\Omega, \quad (6)$$

$$\int_\Omega \frac{du}{dx} w d\Omega + \int_\Omega \frac{dv}{dy} w d\Omega = 0, \quad (7)$$

$$\int_\Omega \frac{DT}{Dt} w d\Omega = -\frac{1}{RePr} \int_\Omega (\nabla T \cdot \nabla w) \, d\Omega. \quad (8)$$

3.2 The Galerkin Method

The Galerkin Method consists of an approximation of the continuous variable to a discrete representation. Then, the shape functions N are used, in order to interpolate the values in the nodes seen in Figure 1, where the MINI and the quadratic elements are presented.

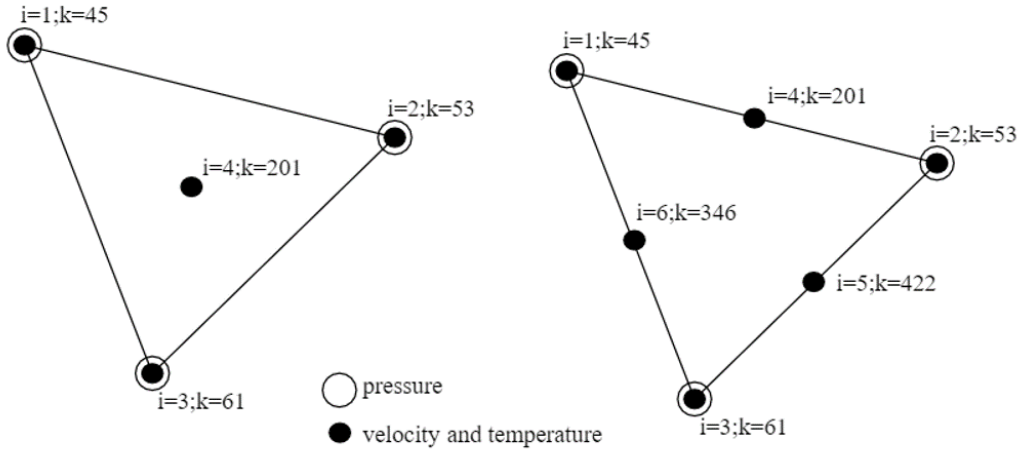

Figure 1: Element's nodes representation, with local (i) and respective global (k) numbers, for MINI (left) and quadratic (right) elements.

Given the elements, the entire mesh is composed of a set of triangular elements, with a total of NP_{total} points, for which the velocities u and v and the temperature are calculated, and NV_{total} vertices, where pressure is associated. The element shown satisfies the LBB condition and the difference between NV and NP is that NV does not account for the midpoints, seen in Figure 1. The variables of interest and their respectful weight functions $\mathbf{w}$, q and r are presented next:

$$u \approx \sum_{i=1}^{NP} N_i(x,y) u_i, \quad v \approx \sum_{i=1}^{NP} N_i(x,y) v_i, \quad p \approx \sum_{i=1}^{NV} L_i(x,y) p_i, \quad T \approx \sum_{i=1}^{NP} N_i(x,y) T_i, \quad (9)$$

$$\mathbf{w} \approx \sum_{j=1}^{NP} N_j(x,y) \mathbf{w}_j, \quad q \approx \sum_{j=1}^{NV} L_j(x,y) q_j, \quad r \approx \sum_{j=1}^{NP} N_j(x,y) r_j. \quad (10)$$

Substituting the approximated variables, as well as the weight approximated forms, into the governing equations and using the index notation leads to:

$$\sum_e \int_{\Omega_e} \frac{DN_i u_i}{Dt} N_j w_{x_j} d\Omega + \frac{1}{ReDa} \sum_e \int_{\Omega_e} \varphi_e \varepsilon_e (N_i u_i + \varphi Fo |\mathbf{u}|_i N_i u_i) N_j w_{x_j} d\Omega - \sum_e \int_{\Omega_e} \frac{\partial N_i w_{x_i}}{\partial x} L_j p_j d\Omega + \frac{1}{Re} \sum_e \int_{\Omega_e} \left(\nabla N_i u_i \cdot \nabla N_j w_{x_j} \right) d\Omega - \sum_e \int_{\Omega_e} \frac{1}{Fr^2} N_i g_{x_i} N_j w_{x_j} d\Omega = 0, \quad (11)$$

$$\sum_e \int_{\Omega_e} \frac{DN_i v_i}{Dt} N_j w_{y_j} d\Omega + \frac{1}{ReDa} \sum_e \int_{\Omega_e} \varphi_e \varepsilon_e (N_i v_i + \varphi Fo |\mathbf{u}|_i N_i v_i) N_j w_{y_j} d\Omega - \sum_e \int_{\Omega_e} \frac{\partial N_i w_{y_i}}{\partial y} L_j p_j d\Omega + \frac{1}{Re} \sum_e \int_{\Omega_e} \left(\nabla N_i v_i \cdot \nabla N_j w_{y_j} \right) d\Omega - \sum_e \int_{\Omega_e} \frac{1}{Fr^2} N_i g_{y_i} N_j w_{y_j} d\Omega = 0, \quad (12)$$

$$\sum_e \left(\int_{\Omega_e} L_i q_i \frac{\partial N_j u_j}{\partial x} d\Omega + \int_{\Omega_e} L_i q_i \frac{\partial N_j v_j}{\partial y} d\Omega \right) = 0, \quad (13)$$

$$\sum_e \left(\int_{\Omega_e} \frac{DN_i T_i}{Dt} N_j r_j d\Omega + \frac{1}{RePr} \int_{\Omega_e} \left(\nabla N_i T_i \cdot \nabla N_j r_j \right) d\Omega \right) = 0, \quad (14)$$

Since w_j appears on both sides of all the equations, it may be eliminated. Grouping and rearranging the terms, the matrices of the linear systems are presented as follows.

$$\mathbf{M} = \sum_e \left(\int_{\Omega_e} \mathbf{N}^T \mathbf{N} d\Omega \right), \quad \mathbf{K} = \sum_e \left(\int_{\Omega_e} \nabla \mathbf{N}^T \nabla \mathbf{N} d\Omega \right), \quad (15)$$

$$\mathbf{G}_x = \sum_e \left(\int_{\Omega_e} \frac{\partial \mathbf{N}^T}{\partial x} \mathbf{L} d\Omega \right), \quad \mathbf{G}_y = \sum_e \left(\int_{\Omega_e} \frac{\partial \mathbf{N}^T}{\partial y} \mathbf{L} d\Omega \right). \quad (16)$$

Finally, the coupled linear system for pressure and velocity, adding the terms of the Darcy/Forchheimer equation, may be written:

$$\begin{bmatrix} \frac{\mathbf{M}}{\Delta t} + \frac{\mathbf{K}}{Re} + \frac{1}{ReDa} \left(\mathbf{M}_\varphi + \mathbf{M}_{\varphi^2} Fo \mathbf{U} \right) & \mathbf{0} & -\mathbf{G}_x \\ \mathbf{0} & \frac{\mathbf{M}}{\Delta t} + \frac{\mathbf{K}}{Re} + \frac{1}{ReDa} \left(\mathbf{M}_\varphi + \mathbf{M}_{\varphi^2} Fo \mathbf{U} \right) & -\mathbf{G}_y \\ \mathbf{D}_x & \mathbf{D}_y & \mathbf{0} \end{bmatrix} \begin{bmatrix} u \\ v \\ p \end{bmatrix} = \begin{bmatrix} \frac{\mathbf{M}}{\Delta t} u_d + \frac{\mathbf{M}}{Fr^2} g_x \\ \frac{\mathbf{M}}{\Delta t} v_d + \frac{\mathbf{M}}{Fr^2} g_y \\ \mathbf{0} \end{bmatrix}. \quad (17)$$

Here, $\mathbf{U}$ and is the diagonal matrix of the modulus of the velocity at the previous time step in each point of the discrete domain, $\mathbf{M}_\varphi$ is the mass matrix considering the ε and φ values of each element, and $\mathbf{M}_{\varphi^2}$, the mass matrix considering an extra φ value of each element, correspondent to the velocity modulus term. Also, $\mathbf{D}_x = \mathbf{G}_x^T$ and $\mathbf{D}_y = \mathbf{G}_y^T$. The

temperature is calculated from a separate linear system, as follows:

$$\left[\frac{1}{\Delta t}\mathbf{M} + \frac{1}{RePr}\mathbf{K}\right]\left[T\right] = \left[\frac{1}{\Delta t}\mathbf{M}T_d\right]. \tag{18}$$

4 THE SEMI-LAGRANGIAN FORMULATION

After discretizing the spatial derivatives through the finite element method, time derivatives must be discretized as well. Since the material derivative of the velocity results in a non-linear term, a lagrangian approach for that term is used, considering a generic variable ψ, that can either be u, v or T. The semi-lagrangian formulation is, then:

$$\frac{D\psi}{Dt} \approx \frac{\psi - \psi_d}{\Delta t}, \tag{19}$$

where the subscript d denotes the variable's value at the previous time step in the location the fluid particle occupied (x_d) at that time. Figure 2 explains how the semi-lagrangian method is made and shows an example of mesh used in this method.

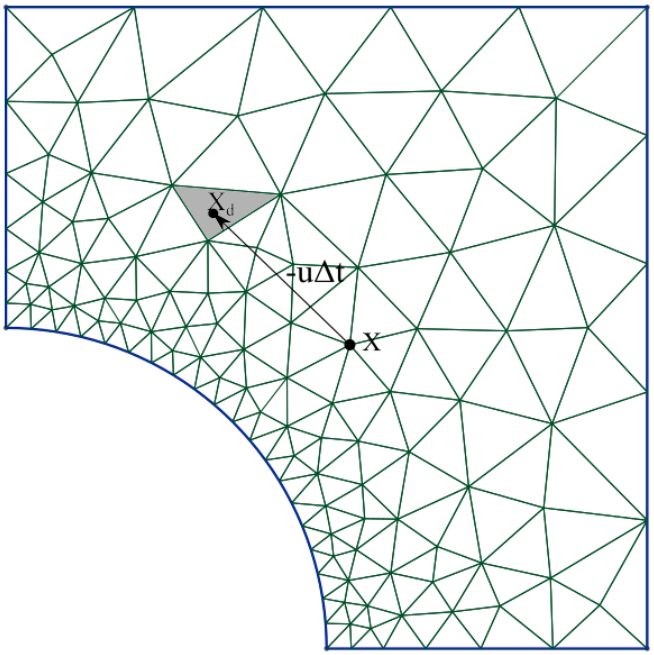

Figure 2: Mesh example and schematic of the semi-lagrangian formulation, where $\mathbf{X}_d$ is the position the fluid particle occupied at the previous time, determined by means of the velocity $\mathbf{u}$ and the time step Δt.

After determining the position $\mathbf{x}_d = \mathbf{x} - \mathbf{u}\Delta t$ of each point in the mesh, including the centroids/midpoints, the variables u_d, v_d and T_d are calculated by means of the interpolation of such variable's value in the points of the element. Note that all available element nodes are used to interpolate the variables, therefore a high-order interpolation scheme is ensured.

5 RESULTS

5.1 The Lid-driven Cavity

The benchmark used to analyze the formulation is the lid-driven cavity problem, where the upper boundary of a rectangular enclosure moves with constant horizontal velocity. This induces a velocity field along the cavity, as can be seen in Figure 3, for $Re = 100$. For this case $1/Fr^2 = 10^{-4}$, where $Fr = U/\sqrt{gL}$ is the Froude number. The mesh used has 3124 elements and 1563 vertices.

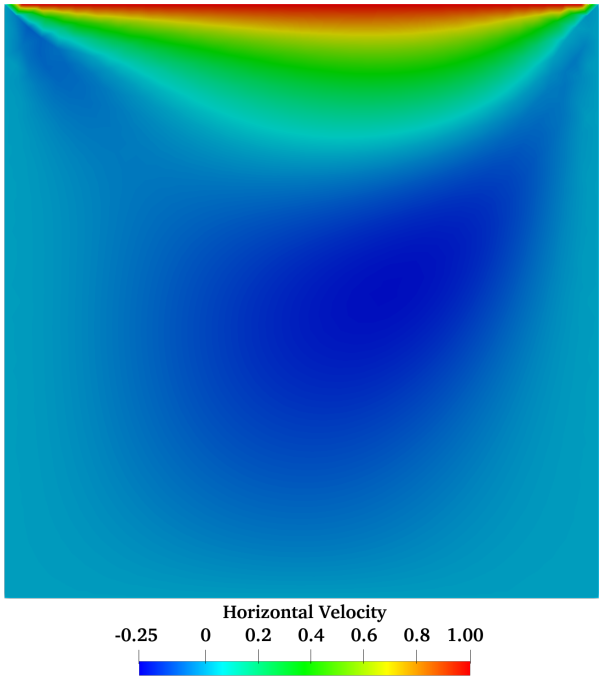

Figure 3: Velocity fields in the horizontal direction for the lid-driven cavity problem, with $Re = 100$.

The velocity fields along the vertical and horizontal lines that pass through the midpoint of the square domain are compared to the results seen in da Cunha (2020). Figure 4 shows the comparison between the current work and the literature, for the MINI and the quadratic formulations.

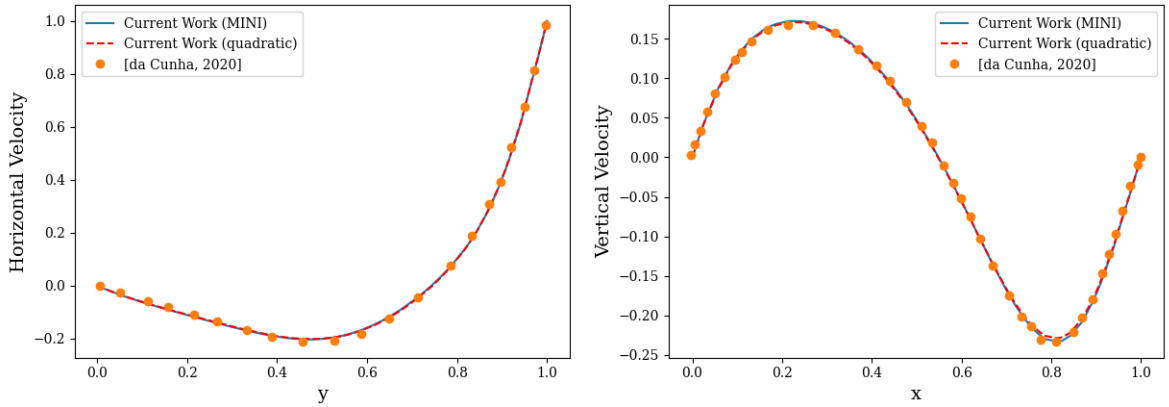

Figure 4: Validation of the lid-driven cavity problem, for velocity components obtained from the central lines crossing the domain, as seen in (da Cunha, 2020).

The result presented is double-validated, since da Cunha (2020) also validates his simulation with the literature, and shows that the implementation in this work was adequate.

5.2 The Flow in a Conjugated Region

After validating the code generated, the flow in a conjugated region is presented, where a fully developed profile is established at the entrance. In this problem, the ε values vary from 0 to 1 in the middle of the domain, where the porous region starts. The simulation was made using a quadratic element mesh, with 4200 elements and a total of 8167 points. In Figure 5, one can notice the transition between regions since the velocity profile in the porous region has a lower peak. For this case, $Re = 100$, $1/Fr^2 = 10^{-4}$, $Da = 10^{-3}$ and $Fo = 2.0$.

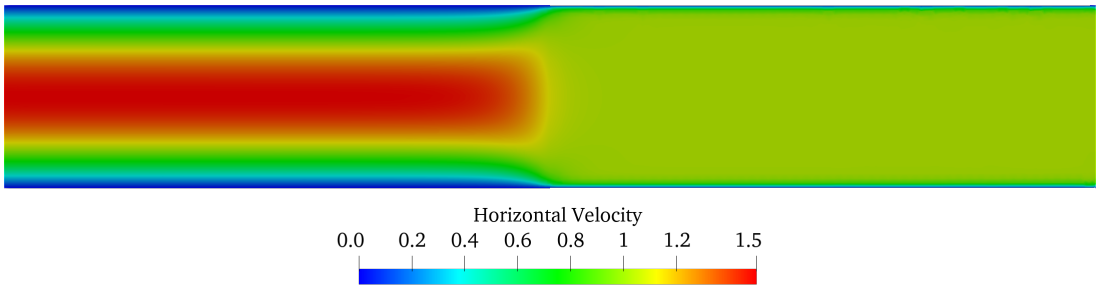

Figure 5: Horizontal velocity field in conjugated flow, with $Re = 100$, $1/Fr^2 = 10^{-4}$, $Da = 10^{-3}$ and $Fo = 2.0$.

Also, heating is provided from a constant surface temperature, with $Pr = 0.7$, resulting in Figure 6.

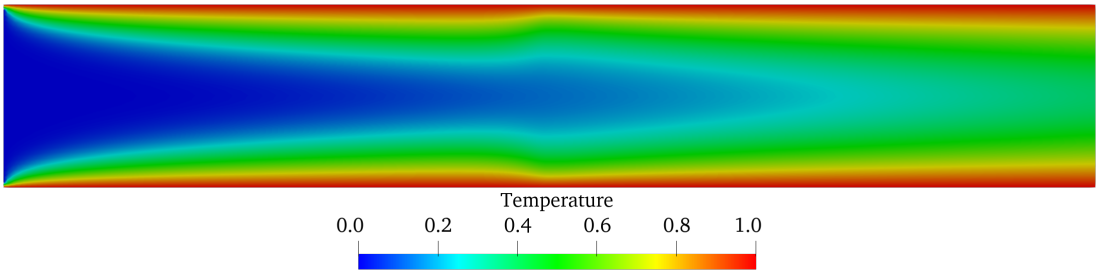

Figure 6: Temperature field in conjugated flow, with $Pr = 0.7$.

It is noticeable that the convective phenomena suffer influence from the media, since the velocity profile changes in the interface of the regions. Hence, the energy transportation throughout the channel is different in said regions. To show that the porous media alters the pressure gradient, which is strictly related to the velocity profile through the momentum equation, we present, in Figures 6 and 8, respectively, the mean-line pressure and velocity.

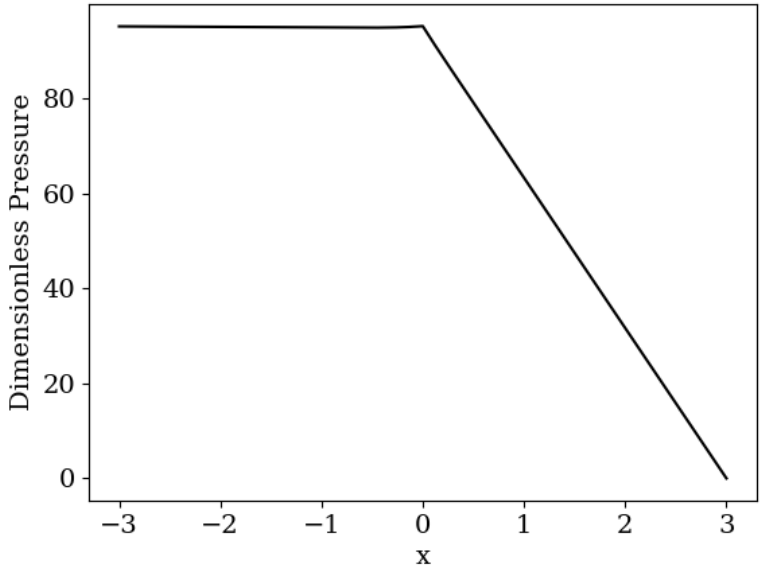

Figure 7: Mean-line pressure in the conjugated flow.

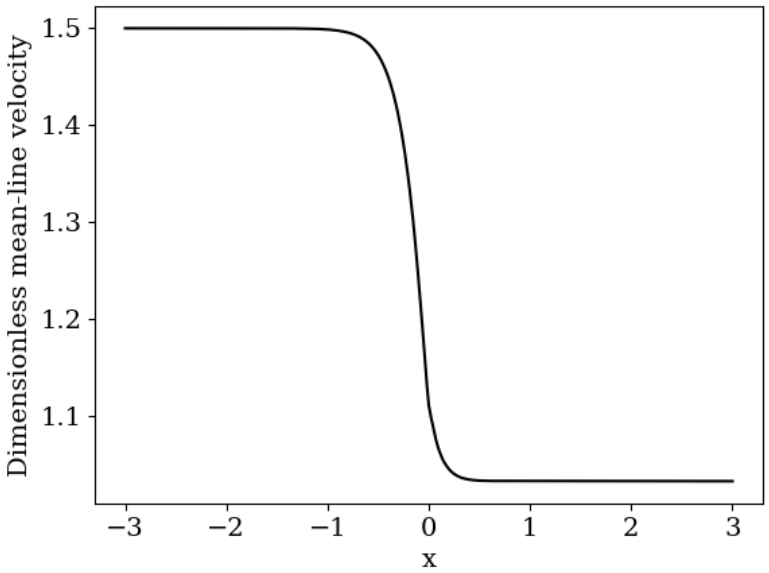

Figure 8: Mean-line velocity in the conjugated flow.

The value of 1.5 for the mean-line velocity proves is in complete accordance with the literature, Batchelor (2000), for a flow between two flat plates. Then, when reaching the porous region, the pressure gradient increases and the velocity profile becomes flatter. Since the mean velocity has to be kept constant, due to mass conservation, the peak velocity is reduced to about 1.0.

This way, the Darcy/Forchheimer equation represents the phenomena of triggering between two regions of different porosity values, providing a good and smooth interface between them.

6 CONCLUSION

This work presented a literature review on numerical methods for free and conjugated flows. Then, the Dary/Forchheimer equation was introduced to represent the said phenomenon. The discretization was made with the finite-element method for momentum, energy and continuity equations, with a semi-Lagrangian technique for the material derivative of velocity fields.

A code verification was made using the well-known lid-driven cavity problem, compared with the literature. Then the conjugated flow was simulated, showing that, for free flow, the value of the mean velocity corresponds to the analytical solution. Also, since the resistance imposed in the porous medium is higher, the pressure drop is steeper, for the same mean velocity. As for the temperature field, it can be noticed that there is a difference between the two regions since convection is affected by the porous domain. Hence, since the transition between regions is smooth, the code is shown to be adequate.

7 ACKNOWLEDGMENTS

The authors would like to thank FAPERJ and CAPES for their financial support.

8 REFERENCES

Abdelwahed, M., Chorfi, N. and Hassine, M., 2011. "A stabilized finite element method for stream function vorticity formulation of navier-stokes equations". *Electronic Journal of Differential Equations*, Vol. 2017, No. 24, pp. 1–10.

Batchelor, G.K., 2000. *An Introduction to Fluid Dynamics*. Cambridge University Press, USA.

Bessaih, H., Garrido-Atienza, M.J. and Schmalfuß, B., 2018. "On 3d navier–stokes equations: Regularization and uniqueness by delays". *Physica D*. doi:https://doi.org/10.1016/j.physd.2018.03.004.

Cimolin, F. and Discacciati, M., 2013. "Navier–stokes/forchheimer models for filtration through porous media". *Applied Numerical Mathematics*, Vol. 72, pp. 205–224. doi:https://doi.org/10.1016/j.apnum.2013.07.001.

da Cunha, L.H.C., 2020. *Ale Finite Element Method for Simulating Flowswith the Stream Function-Vorticity Formulation*. Master's thesis, Mech. Eng. Program of Universidade do Estado do Rio de Janeiro.

Mesquida, I.M.V., 2019. *Analysis of Flow Pattern in a Gasoline Particulate Filter using CFD*. Master's thesis, Chemical and Materials Engineering - University of Alberta.

Souza, J.P.I. and Anjos, G.R., 2023. "A fnite element analysis of multiphase conjugated fow in diesel and biodiesel-driven engine fltration device". *The Brazilian Society of Mechanical Sciences and Engineering*, Vol. 45. doi:10.1007/s40430-023-04295-7.

Toro, L., Cardona, C.A., Pisarenko, Y.A. and Frolkova, A.V., 2018. "The finite element method (fem): An application to fluid mechanics and heat transfer". *Fine Chemical Technologies*, Vol. 13, No. 4. doi:10.32362/2410-6593-2018-13-4-17-25.

Zienkiewicz, O.C. and Taylor, R.L., 2000. *The Finite Element Method - Volume 3*. Wiley.

9 RESPONSIBILITY NOTICE

The authors are solely responsible for the printed material included in this paper.